Publisher homepage: www.universepg.com, ISSN: 2663-7804 (Online) & 2663-7790 (Print)

https://doi.org/10.34104/ajeit.023.01190129

Australian Journal of Engineering and Innovative Technology

Journal homepage: www.universepg.com/journal/ajeit

Development of Graphene with Tungsten Disulfide Composite Layer Based SPR Biosensor for Biomedical Application

Md. Rakibuzzaman Naim[1]*, Nazmul Hossain[1], Munira Islam[1], and Saikat Mitra[1]

[1]Department of Electrical & Electronic Engineering, Khwaja Yunus Ali University, Sirajganj-6751, Bangladesh.

*Correspondence: mdnazmulhossain7890@gmail.com (Nazmul Hossain, Dept. of Electrical & Electronic Engineering, Khwaja Yunus Ali University, Sirajganj-6751, Bangladesh).

ABSTRACT

Surface Plasmon Resonance (SPR) biosensors have been widely used for biomedical applications due to their high sensitivity and label-free detection capabilities. However, their performance can be further enhanced by using advanced materials and signal-processing techniques. The objective of this study is to develop a composite layer-based SPR biosensor using Au, WS2, and Graphene layers and signal processing with MATLAB for enhanced sensitivity and the detection of DNA-DNA Hybridization. The composite layer-based SPR biosensor was fabricated by depositing a thin layer of Au on a glass substrate, followed by the deposition of WS2 and Graphene layers using a Chemical Vapor Deposition (CVD) technique. A self-assembled monolayer of 3-Mercaptopropionic Acid (MPA) was then attached to promote DNA immobilization. The performance of the biosensor was evaluated by detecting the hybridization of a single-stranded DNA (ssDNA) probe with a complementary ssDNA target. The sensor response was analyzed using MATLAB to enhance the sensitivity of the biosensor. The developed composite layer-based SPR biosensor exhibited a highs ensitivity of 592 deg./RIU for the detection of DNA-DNA hybridization. 32.74% sensitivity has been increased. The signal processing with MATLAB significantly improved the signal-to-noise ratio and allowed for real-time monitoring of the biomolecular interactions. The composite layer-based SPR biosensor developed in this study demonstrated enhanced sensitivity for the detection of DNA-DNA hybridization in biomedical applications. The use of advanced materials such as Au, WS2, and Graphene layers, coupled with signal processing with MATLAB, can significantly improve the performance of SPR biosensors. This biosensor has great potential for use in various areas, including genetic testing, drug discovery, and disease diagnosis. Detected DNA-DNA hybridization is used in the biomedical field to identify and classify microorganisms by comparing the degree of genetic similarity between their DNA sequences.

Keywords: SPR, ATR, dsDNA, R_{min}, Tungsten disulfide, Composite layer, T_{max}, RFC, Graphene, and WS_2.

INTRODUCTION:

Surface Plasmon Resonance (SPR) is a powerful analytical technique used to study biomolecular interactions in real time without the need for labels or tags. It is based on the principle of detecting changes in refractive index that occur at a thin metal film surface when biomolecules bind to it. SPR has become an essential tool for drug discovery, biosensor development, and fundamental studies of molecular recognition. The basic principle of SPR is that a light wave can excite oscillations of free electrons (plasmons) at the interface of a metal and a dielectric medium (usually glass). These plasmons can then interact with the incident light, leading to a reduction in the reflected light intensity at a specific angle, known as the resonance angle. When biomo-

lecules bind to the metal surface, they cause a change in the local refractive index, which alters the angle at which resonance occurs. This change in resonance angle is proportional to the number of bound biomolecules, allowing for real-time monitoring of the binding kinetics. SPR can be used to determine various parameters of biomolecular interactions, such as affinity, kinetics, and thermodynamics. It can also be used for high-throughput screening of small molecules and antibodies for drug discovery. SPR has been widely applied in many fields, including biotechnology, biochemistry, and materials science (Homola *et al.,* 1999). SPR has found applications in drug discovery, proteomics, genomics, and other areas of life science research. For example, it has been used to study protein-protein interactions, small molecule binding, and antibody-antigen interactions. Recently, SPR has also been applied to the study of extracellular vesicles (EVs), which are small, membrane-bound particles that are secreted by cells and play important roles in intercellular communication.

In a recent study, researchers used SPR to study the interactions between EVs and cancer cells. They immobilized EVs on the SPR sensor surface and measured the binding of cancer cells to these EVs in real time. They found that the binding of cancer cells to EVs was dependent on the type of EVs and the cancer cell line, suggesting that EVs may play a role in cancer progression through cell-cell communication. This study demonstrates the potential of SPR as a tool for studying EV biology and for developing the new cancer therapies (Nishat *et al*., 2021; Wang *et al.,* 2021).

METHODOLOGY:

The performance parameter descriptions. SPR sensor performance analysis terms such as Surface Plasmon Resonance Angle (θ_{SPR}), SPR frequency, minimum reflectance, maximum transmittance, SPR wavelength, and sensitivity analysis are defined by their mathematical identity.

Surface plasmon resonance angle (θ_{SPR})

At the SPR curve, under resonant conditions, the excitation of surface plasmon polariton (SPP) is known as the minimum total reflectance (i.e., ATR minimum). The angle of incidence at which ATR minimum occurs is called the SPR angle (Vukusic *et al.,* 1992), which can be expressed in (Kruchinin *et al.,* 1996) as shown in the equation below:

$$\theta_{SPR} = \sin^{-1}\sqrt{\frac{n_{Au}^2\, n_s^2}{n_P^2\,(n_{Au}^2 + n_s^2)}} \qquad \ldots\ldots\ldots (1)$$

The SPR angle, as shown in **Fig. 1** above, has a value of 74.293 degrees for the bare sensor without the Graphene structure. The SPR curve was obtained through MATLAB-18 simulation at a wavelength of 633 nm. The refractive index (RI) of the sensing medium has a significant influence on the reflectance and SPR angle (Kruchinin *et al.,* 1996).
The performance parameters of the SPR sensor are mainly evaluated based on its sensitivity, detection accuracy, and quality factor. The sensitivity (S), detection accuracy, and quality factor are directly proportional to the shift in the SPR angle ($\Delta\theta_{SPR}$). The SPR angle plays an active role in determining whether successful interaction is detected in the sample or not, as shown in **Table 1**.

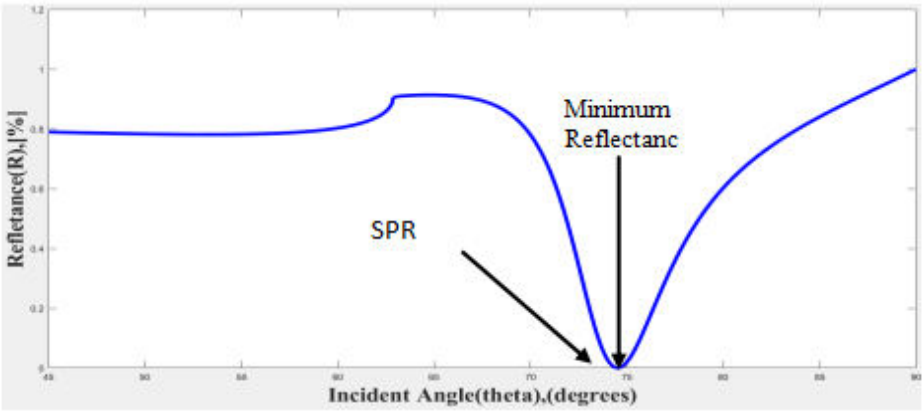

Fig. 1: SPR angle simulating with hybrid layer

Table 1: Conditions for making a decision about successful detection using $\Delta\theta_{SPR}$ and R_{min}.

Conditions for using and R_{min} as detecting attributor	Decision
$\triangle R_{min}^{P-T} \geq (\triangle R_{min}^{P-T})_{min}$ && $\triangle \theta spr^{P-T} \geq (\triangle \theta spr^{P-T})_{min}$	Sample is detected
$\triangle R_{min}^{P-T} \geq (\triangle R_{min}^{P-T})_{min}$ && $\triangle \theta spr^{P-T} \leq (\triangle \theta spr^{P-T})_{min}$	Re-evaluate
$\triangle R_{min}^{P-T} \leq (\triangle R_{min}^{P-T})_{min}$ && $\triangle \theta spr^{P-T} \geq (\triangle \theta spr^{P-T})_{min}$	Re-evaluate
$\triangle R_{min}^{P-T} \leq (\triangle R_{min}^{P-T})_{min}$ && $\triangle \theta spr^{P-T} \leq (\triangle \theta spr^{P-T})_{min}$	Free Probe

Where, $\triangle R_{min}^{P-T}$ is the threshold value of changing reflectance, $\triangle \theta spr^{P-T}$ is the threshold value of changing the SPR angle, $(\triangle R_{min}^{P-T})_{min}$ is the threshold value of changing minimum reflectance and $(\triangle \theta spr^{P-T})_{min}$ is the threshold value of changing the minimum SPR angle. These numerical values can indicate successful or unsuccessful interactions. The first condition in **Table 1** represents the desired outcome, while the second and third conditions require careful review to achieve the desired result. The fourth condition confirms that the probe is still free from DNA molecules.

Minimum reflectance (R_{min})

The incident light is generated an evanescent wave when passes through the prism and it is reflected at the prism-gold interface. The reflection intensity for TM-polarized light is expressed as:

$$R = \frac{A + \frac{B}{Z_f} - Zi\,(C + \frac{D}{Z_f})}{A + \frac{B}{Z_f} + Zi\,(C + \frac{D}{Z_f})} \quad \ldots\ldots(2)$$

The reflectance at the SPR angle is called Minimum Reflectance (R_{min}). The SPR curve is shown in the above **Fig. 1**. The value of Minimum Reflectance (R_{min}) is 0.21992 %. The R_{min} also plays an active role in making decisions about whether successful interaction either sampled is detected or not as shown in **Table 2**.

Surface resonance frequency (SRF)

The intersection of the optical wave propagation constant and the surface plasmon wave propagation constant, referred to earlier, is designated as the Surface Resonance Frequency (SRF) (Kruchinin *et al.,* 1996). As per Equation 3, the SPR angle is a dependent parameter on the refractive index of the sensing medium. It's worth noting that the frequency at which the surface plasmon wave propagates at the SPR point is known as the Surface Resonance Frequency (SRF), as described in the following equation:

$$SRF = \frac{C_0}{n_{geo}} \frac{K_{spw}}{2\pi} \quad \ldots\ldots(3)$$

As per Equation 3, the SPR angle is contingent upon the refractive index of the sensing medium, as well as the propagation velocity of the surface plasmon wave (SPW), which is an evanescent electromagnetic wave that is confined perpendicularly. n_{geo} is the geometric mean of the interface between gold and sensing medium ($n_{geo}=\sqrt{(n_{Au}\, n_s\, n_{prism})}$), omitting imaginary part that is essential to real-world design (Wang Y., & Irudayaraj J. 2012). Here it works on a real surface but its imaginary portion comes into action for sensor designing as surface plasmon wave propagates along the interface between metal and sensing medium (dielectric). The SRF is shown in **Fig. 2**. The value of SPR frequency for the above SPR curve is 110.4547 THz. The SRF curve has been achieved by MATLAB-18, simulating at 633 nm wavelength light. The SRF also plays an active role in making decisions about successful interactions whether sampled is detected or not as shown in **Table 2**.

Table 2: Conditions for making a decision about successful detection using ΔSRF and T_{max}.

Conditions for using ΔSRF & T_{max} as detecting attributor	Decision
$\triangle T_{max}^{P-T} \geq (\triangle T_{max}^{P-T})_{min}$ && $\triangle SRF_{p-t} \geq (\triangle SRF_{p-t})_{min}$	Sample is detected
$\triangle T_{max}^{P-T} \geq (\triangle T_{max}^{P-T})_{min}$ && $\triangle SRF_{p-t} \leq (\triangle SRF_{p-t})_{min}$	Re-evaluate
$\triangle T_{max}^{P-T} \leq (\triangle T_{max}^{P-T})_{min}$ && $\triangle SRF_{p-t} \geq (\triangle SPRF_{p-t})_{min}$	Re-evaluate
$\triangle T_{max}^{P-T} \leq (\triangle T_{max}^{P-T})_{min}$ && $\triangle SRF_{p-t} \leq (\triangle SRF_{p-t})_{mim}$	Free Probe

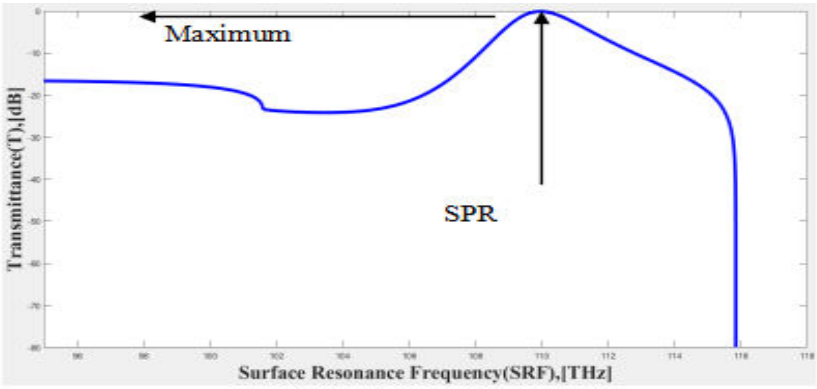

Fig. 2: SPR frequency simulating with hybrid layer.

Where, $\triangle T_{max}^{P-T}$ is the threshold value of changing transmittance, $\triangle SRF_{p-t}$ is the threshold value of changing surface resonance frequency, $(\triangle T_{max}^{P-T})_{min}$ is the threshold value of changing minimum transmittance and $(\triangle SRF_{p-t})_{min}$ is the threshold value of changing minimum surface resonance frequency.

These acquired numerical values can give an option about successful interactions or failed ones. The first condition in **Table 3** expresses the desired condition, the second and third ones require careful rechecks for attaining the desired condition, and the fourth condition confirms the probe is still free from the sample molecule.

Maximum transmittance (T_{max})

The transmitted light can be determined by equation (4):

$$T = \frac{2\cos\theta_i}{A + \frac{B}{Z_f} + Zi\,(C + \frac{D}{Z_f})\cos\theta_f} \qquad \ldots\ldots(4)$$

The transmittance at SPRP is called Maximum Transmittance (T_{max}) (Jonsson *et al.,* 2007). For resonance conditions the maximum transmittance is necessary. The result is expressed in decibel (dB) (Aslan *et al.,* 2005). The SPR curve is shown in the below **Fig. 7**. The value of Maximum Transmittance (T_{max}) is -1.223 dB. The T_{max} also plays an active role in making decisions about whether successful interaction either the sampled is detected or not as shown in **Table 2**.

Detection flowchart (based on matlab & Table 2 & 3 conditions)

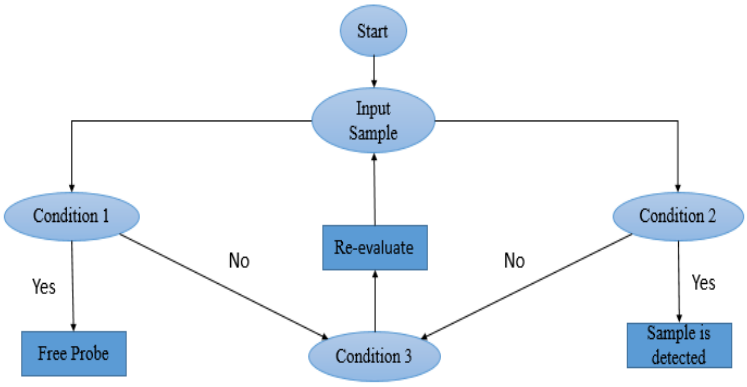

Flow Chart: Transmittance/Reflectance Based Bio-medical Application

Sensitivity analysis

The sensitivity of SPR-sensing devices has been widely studied (Tubb *et al.,* 1997). The sensitivity of SPR angular interrogation-based sensors to changes in the refractive index has been found to increase with decreasing operation wavelength, conversely, the sensitivity of SPR refractive index sensors using wavelength interrogation and intensity measurement increases with the wavelength (Earp *et al.,* 1998). The sensitivity of the optical SPR sensor is defined as the ratio of the change of output parameters (SRF, θ_{SPR}) to the change in concentration of biomolecules, Δca (sensor input/biomolecule concentration) as given below:

$$S = \frac{\Delta\theta}{\Delta Ca} \quad \text{or} \quad S = \frac{SRF}{\Delta Ca} \qquad \text{……(5)}$$

Where, S is the sensor sensitivity.
We can also find sensitivity using equation 6

$$S = \frac{\partial\theta}{\Delta n} \qquad \text{……(6)}$$

Where the resonance angle ($\delta\theta$) and the RI change in sensing region (Δn)

RESULTS AND DISCUSSION:

The main performance parameters of the SPR sensor are sensitivity, detection accuracy and the quality factor, all of which should be as high as possible for a good sensor. The sensitivity (S) to the sensing region refractive index change is defined as the ratio of shift in the ratio of shift in the resonance angle of incidence (δ) to the RI change in the sensing region (δ);

$$S = \frac{\delta\theta}{\Delta n} \qquad \text{……(7)}$$

The variation of the reflection intensity in accordance with the incidence angle is plotted in **Fig. 3**. The reflectance curves at 1.350 RI and 1.354 RI of sensing layer are presented by solid lines of different colors respectively.

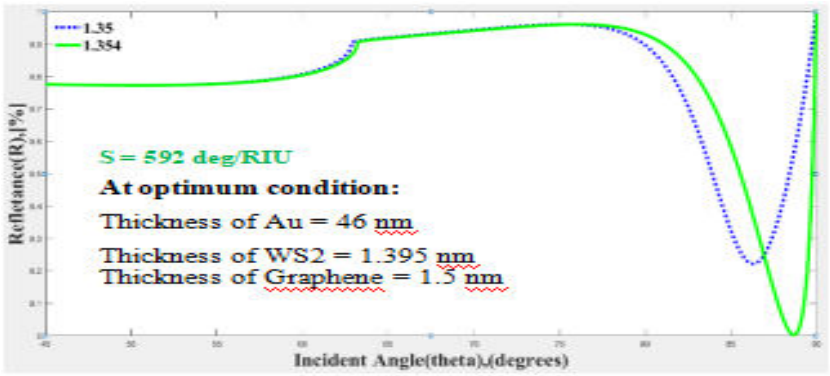

Fig. 3: Reflectivity vs incident angle.

Here the proposed structure RI range (1.33 to 1.375) is used. The structure has the highest resonance angle, which ranges from 86.33° to 88.7°. 1.354 manifests the maximum resonance angle of 88.7°. This result confirms the validity of the suggested model based on Au, WS_2 and Graphane One can easily observe from the **Fig. 3** that the sensitivity increases gradually with the adde1d layers and be the maximum with the hybrid structure of five layers (proposed structure).

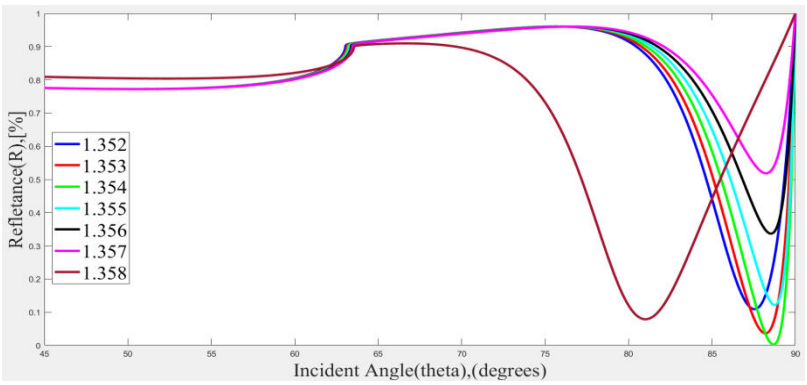

Fig. 4: Reflectance vs incident angle curve for different concentration of detectable target.

Here, 1.354 RI in figure shows the lowest reflectance.

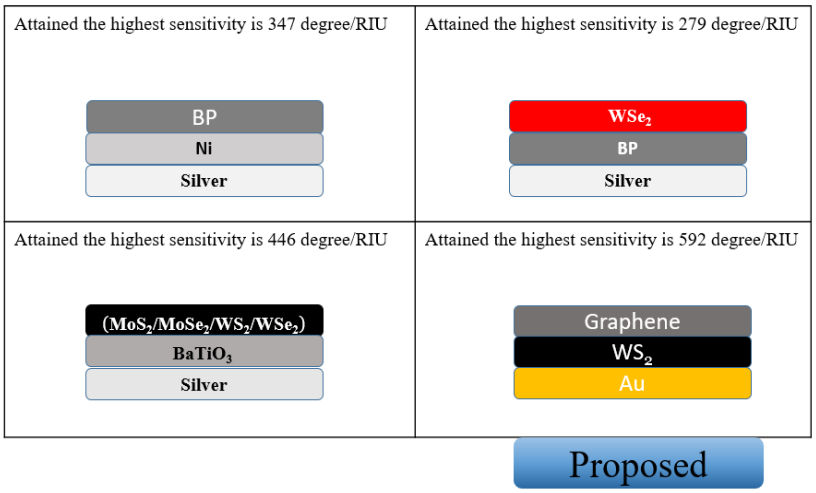

Fig. 5: Different reported prism based SPR biosensors sensitivity comparison.

Fig. 5 presents a comparison of the previously published data with the proposed models. The table demonstrates that the suggested sensor has a greater sensitivity than prior works.

Minimum reflectance (R_{min}) and SPR angle attributors

Fig. 6 illustrates DNA hybridization, where two complementary single-stranded DNAs, one being a probe and the other being the target, form a double-stranded helix structure. This event is called a complementary hybridization. The proposed model in this chapter explains the sensor's analytical behavior to detect the hybridization of target DNAs to the probe DNAs immobilized on the graphene. The detection process begins by analyzing the reflection angle (R~θ) of the incident characteristic before adding DNA molecules, also known as naked sensors, as illustrated in **Fig. 6**. The SPR device is used to measure the dependence of reflectance on the incident angle. In the following sections, we demonstrate how the refractive index changes with the concentration of DNA, expressed by the given equations (Liedberg *et al.,* 1983).

$$n_s^d = n_s + C_0 \frac{d_n}{d_c} \quad \text{.....(8)}$$

After the adsorption of DNA molecules, the refractive index (RI) of the sensor dielectric changes. The RI of the sensor dielectric before adsorption of DNA molecules is denoted by ns, and ca is the concentration of adsorbed DNA molecules. The parameter dn/dc is the increment of RI due to adsorption, which is dn/dc = 0.182 cm3/g when using an SPR device (Nylander *et al.,* 1982). The propagation constant of the light wave given by Equation 8 is equal to the SP wave at the SPR point, as given by Equation 8. A change in the concentration of the detection medium due to DNA immobilization causes a change in the local RI (ns) of that detection medium, as expressed in Equation 7. From Equation 8, we observe that ksp changes as ns changes. In conclusion, we found that the SPR angle also the changes. The changing properties of the SPR angle with changes in RI are further discussed in Section (SPR Angle). The proposed model explains the analytical behavior of the sensor to detect the hybridization of target DNAs to the probe DNAs immobilized on Graphene. To initiate detection, the incident characteristic reflection angle (R~θ) is analyzed before adding DNA molecules, typically known as naked sensors, as shown in **Fig. 6**.

The dependence of reflectance on an incident angle is measured by the SPR device. First, we demonstrate how the RI varies with changes in molarity. This relationship is expressed by the given equations (Nylander *et al.,* 1982)

$$K_x = \frac{2\pi}{\lambda} n_p \sin\theta \quad \text{.....(9)}$$

$$K_{sp}=\frac{2\pi}{\lambda}\sqrt{\frac{n^{z_m}\ n^{z_s}}{n^{z_m}+n^{z_s}}} \qquad \ldots\ldots\ldots(10)$$

Numerical results

The detection process begins by the analyzing the characteristic reflection angle (R~θ) before introducing the biomedical sample molecule. Our calculations measure the dependence of reflectance on an incident angle using the SPR device (Jorgenson, R. C., & Yee, S. S. 1993). The SPR curve exhibits a bipolar nature, as depicted in **Fig. 4**. At the point of transition where the SPR and optical wave vectors coincide, a minimum reflectance (Rmin) is observed. This decision point is known as the surface plasmon polariton point (SPRP). The SPR curve graphically represents this information.

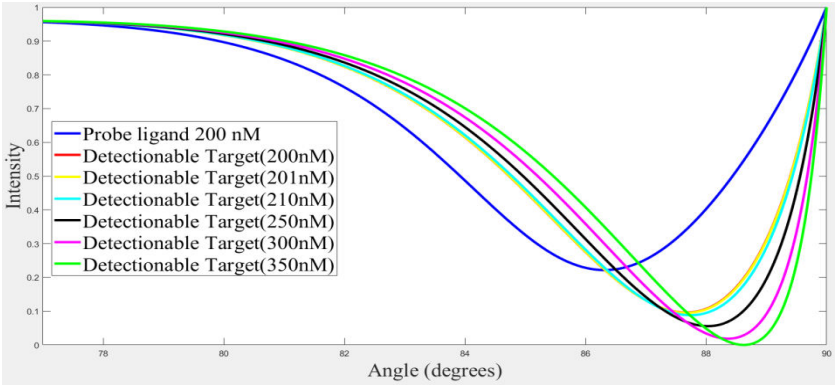

Fig. 6: Reflectance vs incident angle curve for different concentration of detectable target.

Table 3: R_{min}[%] and θsp[deg] for different concentration of dielectric medium.

Concentration(Ca) [nM]	R_{min}[%]	θ_{sp}[deg]
200 (immobilizer probe)	0.22174	86.33
200 (detection able target)	0.09595	87.68
201 (detection able target)	0.09516	87.69
210 (detection able target)	0.088	87.75
250 (detection able target)	0.05563	88.04
300 (detection able target)	0.0185	88.38
350 (detection able target)	0.00002	88.64

Introduction of a probe sample molecule results in the alteration of the refractive index (RI) of the sensor dielectric, which leads to a rightward shift of the SPR angle. Furthermore, adsorption of an electron-rich sample molecule alters the concentration of charge carriers in the Graphene sheet, leading to a modification in the propagation constant. The detection of sample events was ultimately carried out by the introduction of the complementary sequences immobilized on Graphene and SPR devices (Jorgenson, R. C., & Yee, S. S. 1993). As the analytical data in the table show, the magnitude of the shift increases from first 200 nM to 201 nM and second 210 nM to 250 nM with increasing concentration of complementary DNA. The extent of these changes determines whether hybridization occurs in the presence of the complementary or non-complementary DNA.

Table 4: ΔR_{min}^{P-T} [%] and ΔR_{min}^{P-T} [%] for different concentration of dielectric medium.

Concentration(Ca) [nM]	R_{min}^{P-T} [%]=$\left\|R_{min}^{probe} - R_{min}^{terget}\right\|$	$\Delta\theta_{sp}^{P-T}$[deg]=$\left\|\theta_{sp}^{Probe} - \theta_{sp}^{terget}\right\|$
200 (Target)	$(R_{min}^{P-T})_{\min}$	$(\Delta\theta_{sp}^{P-T})_{\min}$
201 (Target)	0.12658	1.36
210 (Target)	0.13374	1.42
250 (Target)	0.16611	1.71
300 (Target)	0.20324	2.05
350 (Target)	0.22172	2.31

Where θ_{sp}^{Probe} the SPR angle of probe DNA molecule is, θ_{sp}^{terget} denotes SPR angle in a specific DNA concentration, R_{min}^{probe} represents the minimum Reflectance of probe DNA molecule while R_{min}^{terget} shows its concentration. Where $\Delta\ \theta_{sp}^{Probe}$ is the small change SPR angle of probe DNA molecule, θ_{sp}^{terget} denotes SPR angle in a specific DNA concentration, ΔR_{min}^{probe} represents the small changes Reflectance of probe DNA molecule while R_{min}^{terget} shows its concentration.

Table 5: Four probable conditions for making decision about successful interaction for DNA-DNA hybridization.

Conditions	Decision
$\Delta R_{min}^{P-T} \geq (\Delta R_{min}^{P-T})_{\min}$ && $\Delta\theta_{sp}^{P-T} \geq (\Delta\theta_{sp}^{P-T})_{\min}$	DNA-DNA Hybridized
$\Delta R_{min}^{P-T} \geq (\Delta R_{min}^{P-T})_{\min}$ && $\Delta\theta_{sp}^{P-T} \leq (\Delta\theta_{sp}^{P-T})_{\min}$	Re-evaluate
$\Delta R_{min}^{P-T} \geq (\Delta R_{min}^{P-T})_{\min}$ && $\Delta\theta_{sp}^{P-T} \leq (\Delta\theta_{sp}^{P-T})_{\min}$	Re-evaluate
$\Delta R_{min}^{P-T} \leq (\Delta R_{min}^{P-T})_{\min}$ && $\Delta\theta_{sp}^{P-T} \leq (\Delta\theta_{sp}^{P-T})_{\min}$	Free Probe

Numerical results of maximum transmittance

To acquire numerical results, the characteristic curves of T~SRF were compared with and without the Graphene under layer before introducing sample molecules, which is typically referred to as a simple sensor. The obtained numerical results acted as a detection medium to aid in determining the dependence of permeation on SRF.

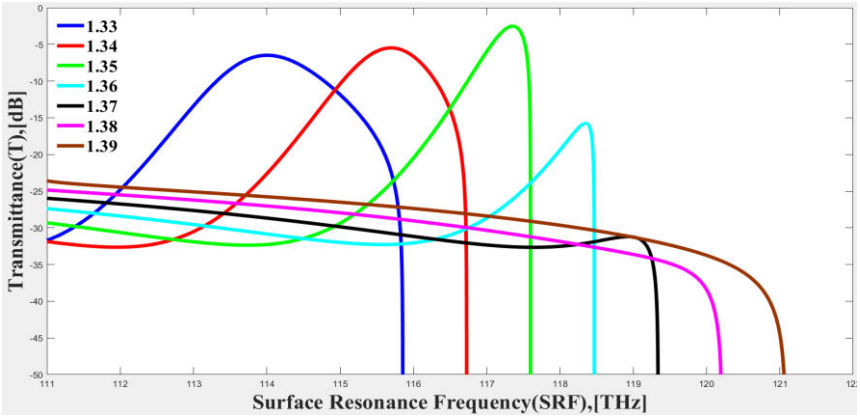

Fig. 7: Variation of the transmittance with respect to the surface resonance frequency.

This phenomenon can demonstrate the dependence of SRF on the immobilization of probe DNA and the hybridization of complementary target DNA (C-t-DNA) (Jorgenson, R. C., & Yee, S. S. 1993). By introducing DNA as an electron-rich molecule, the number of carriers changes the Graphene concentration.

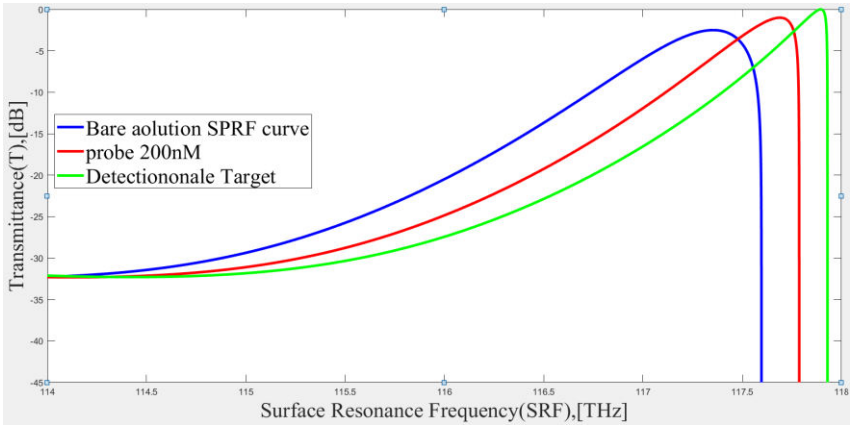

Fig. 8: Comparison of SPRF curve among bare solution, probe ligand and unbounded detectable target.

As shown in **Fig. 8**, when non-complementary t-DNA is immersed in the immobilized capture probes on the SPR device, single base mismatch combinations occur and the T~SRF signature (the SRF angle of change) did not change significantly. Refers to a mismatched target, ΔSRF = 0.1 THz, since there is no binding reaction between the two sets of DNA strands.

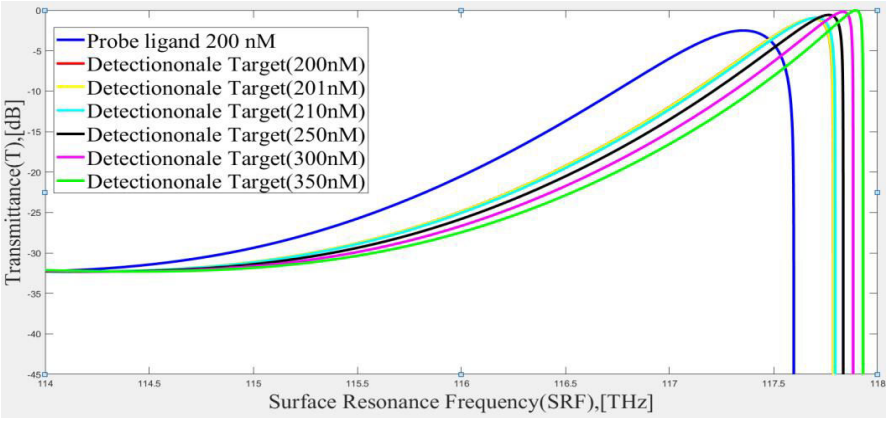

Fig. 9: Transmittance vs SPRF frequency curves for different.

Concentration of detectable target

In this case, we conclude that there is no charge associated with the target molecule that could accompany any apparent change in the applied sensor dielectric. It is also observed that the SPR device specifically recognizes target DNA sequences. Considering this fact, the focus of this paper is to present a new strategy for DNA sensors with the ability to detect SNPs. **Fig. 9** shows the T~SRF profile for various concentrations of complementary target DNA (C-t-DNA). Each colored line represents a finite concentration of DNA molecules. According to numerical data, SRF and T_{max} acted as hybridization detectors. These parameters change and decisions are made based on these changes when a complementary DNA molecule is combined with the probe. SRF and T_{max} were calculated for different concentrations of C-t-DNA and tabulated. By the equation 8 Know how these parameters change when the concentration changes. A significant increase in SRF is indicative of DNA hybridization. Numerical data show a strong dependence of SRF on increasing concentration, which is reflected in the T~SRF curve. During DNA hybridization, C-t-DNA molecules react with the Graphene surface. This is commonly known as the "Graphene – nucleotide interaction" and produces an n-doping effect that easily bends to the right. It has been found that the interaction between nucleotides and the Graphene surface in DNA hybridization also has a profound effect on the SRF, which can alter it to the right (Hutley, C, 1982).

Table 6: T_{max}[dB] and SPRF for different concentration of dielectric medium.

Concentration(C_a) [nM]	**□T_{max} [dB]**	**□SPRF[THz]**
200 (immobilizer probe)	-2.5069	117.3547
200 (detection able target)	-1.0087	117.6898
201 (detection able target)	-0.9999	117.6916
210 (detection able target)	-0.9212	117.7050
250 (detection able target)	-0.5723	117.7650
300 (detection able target)	-0.1868	117.8345
350 (detection able target)	-0.00015862	117.8960

Table 7: ΔT_{max}^{P-T} and ΔSFR_{p-t} for different concentration of dielectric medium.

Conditions for using ΔSRF & T_{max} as detecting attributor	**Decision**
$\triangle T_{max}^{P-T} \geq (\triangle T_{max}^{P-T})_{min}$ && $\triangle SRF_{p-t} \geq (\triangle SRF_{p-t})_{min}$	Sample is detected
$\triangle T_{max}^{P-T} \geq (\triangle T_{max}^{P-T})_{min}$ && $\triangle SRF_{p-t} \leq (\triangle SRF_{p-t})_{min}$	Re-evaluate
$\triangle T_{max}^{P-T} \leq (\triangle T_{max}^{P-T})_{min}$ && $\triangle SRF_{p-t} \geq (\triangle SPRF_{p-t})_{min}$	Re-evaluate
$\triangle T_{max}^{P-T} \leq (\triangle T_{max}^{P-T})_{min}$ && $\triangle SRF_{p-t} \leq (\triangle SRF_{p-t})_{mim}$	Free Probe

Table 8: Four probable conditions for making decision about successful interaction for DNA-DNA hybridization.

Concentration(C_a) [nM]	ΔT_{max}^{P-T}[dB]= $\lvert R_{max}^{P} - T_{max}^{t} \rvert$	ΔSFR_{p-t}[THz]= $\lvert SRF_p - SRF_t \rvert$
200(Target)	$(\Delta T_{max}^{P-T})_{min}$	$(\Delta SFR_{p-t})_{min}$
201(Target)	1.507	0.3369
210(Target)	1.5857	0.3503
250(Target)	1.9346	0.4103
300(Target)	2.3201	0.4798
350(Target)	2.50674138	0.5413

Where, ΔT_{max}^{P-T} is the threshold value of changing transmittance, ΔSRF_{p-t} is the threshold value of changing surface resonance frequency, $(\Delta T_{max}^{P-T})_{min}$ is the threshold value of changing minimum transmittance and $(\Delta SRF_{p-t})_{min}$ is the threshold value of changing minimum surface resonance frequency. Finally taking advantage of the attribute's values, a decision-making **Table 8** is prepared and can be utilized. When the change of ΔSRF and ΔT_{max}^{p-t} is greater than or equal to $(\Delta SRF)_{min}$ (117.3547 THz) and $(\Delta T_{max}^{p-T})_{min}$ (-2.5069 db) then DNA-DNA hybridization has been ensued and if the change of (Δ SRF) and ΔT_{max}^{p-t} is less than $(\Delta SRF)_{min}$ and $(\Delta T_{max}^{p-t})_{min}$ then SNP is happened, except these both case, no effective result will be established, detection procedure should be Re-evaluate.

CONCLUSION:

Graphene nanomaterial possesses exceptional properties such as high surface area, electrical conductivity, and biocompatibility, rendering it a remarkable biosensing material for sample detection. Currently, detecting samples is an area of great interest, given that recent studies have demonstrated the role of gene mutations in numerous inherited human disorders. In this research, we have employed Graphene as both a sensing layer and a conducting channel in solution-gated field effect transistors for detecting DNA-DNA hybridization. To facilitate the rational design and characterization of these devices, we have developed a sample sensor model using particle swarm optimization theory for detecting biomedical samples. Furthermore, our proposed model can identify single-nucleotide polymorphisms by suggesting detective parameters (Ids and Vg min). Finally, we have compared the performance of solution-gated field effect transistor-based Graphene & WS2 through experiment results. Our proposed biosensor comprises a Graphene material sandwiched between metal films sensing medium, which enhances sensor sensitivity. Without Graphene and WS2 sub-layers, surface plasmon resonance sensor provides slower immobilization between target sample and probe sample, resulting in lesser sensitivity and poor efficiency. We have observed that adding each sub-layer increases sensitivity by 32.74% if Surface Resonance Frequency & maximum transmittance are selected as detecting attributors.

ACKNOWLEDGEMENT:

We begin by the expressing our gratitude to the Almighty Allah. We also extend our heartfelt appreciation to our department and teachers provided us with a conducive environment to carry out our research and their contributions were invaluable. We also extend our gratitude to Saikat Mitra, Lecturer in the Dept. of Electrical and Electronic Engineering, Khwaja Yunus Ali University, Sirajganj, Bangladesh, whose contribution to this thesis cannot be overstated.

CONFLICTS OF INTEREST:

The authors declare that they have no competing interest.

REFERENCES:

1) Aslan, K., Gryczynski, I., and Lakowicz, J. R. (2005). Metal-enhanced fluorescence: An emerging tool in biotechnology. *Current Opinion in Biotechnology*, **16**(1), 55-62. https://doi.org/10.1016/j.copbio.2004.11.003
2) Earp, R. L., & Dessy, R. E. (1998). Surface plasmon resonance. In Commercial biosensors: Applications to clinical, bioprocess, and environmental samples (pp. 97-122). *John Wiley and Sons*.
3) Homola, J., Yee, S. S., & Gauglitz, G. (1999). Surface plasmon resonance sensors: review. *Sensors and Actuators B: Chemical*, **54**(1-2), 3-15.
4) Hutley, C. (1982). Diffraction gratings. *London: Academic Press*.

5) Jorgenson, R. C., and Yee, S. S. (1993). A fiber-optic chemical sensor based on surface plasmon resonance. *Sensors and Actuators B*, **12**, 213-220. https://doi.org/10.1016/0925-4005(93)85135-V
6) Kruchinin, A. A., & Vlasov, Y. G. (1996). Surface plasmon resonance monitoring by means of polarization state measurement in reflected light as the basis of a DNA probe biosensor. *Sensors & Actuators B*, **30**, 77-80. https://doi.org/10.1016/0925-4005(96)80016-5
7) Liedberg, B., Nylander, C., & Lundstro¨m, I. (1983). Surface plasmon resonance for gas detection & biosensing. *Sensors and Actuators*, **4**, 299-304.
8) Nishat M, Islam R, and Rahman MA. (2021). Investigation of the effect of 3d TM-TM atom co-doped in graphene nanosheet: DFT based calculations, *Int. J. Mat. Math. Sci*., **3**(6), 122-132. https://doi.org/10.34104/ijmms.021.01220132
9) Nylander, C., Liedberg, B., & Lind, T. (1982). Gas detection by means of surface plasmon resonance. *Sensors and Actuators*, **3**, 79-88. https://doi.org/10.1016/0250-6874(82)85006-1
10) Tubb, A. J. C., Payne, F. P., & Lowe, C. R. (1997). Single mode optical fiber surface plasma wave chemical sensor. *Sensors and Actuators B*, **41**, 71-79. https://doi.org/10.1016/s0925-4005(97)80153-6
11) Vukusic, P. S., Bryan-Brown, G. P., and Sambles, J. R. (1992). Surface plasmon resonance on grating as novel means for gas sensing. *Sensors and Actuators B*, **8**, 155-160. https://doi.org/10.1016/0925-4005(92)80016-A
12) Wang, Y., and Irudayaraj, J. (2012). Surface plasmon resonance: A versatile technique for biosensor applications. *Sensors*, **12**(12), 16507-16528. https://doi.org/10.3390/s121216507
13) Wang, L., Yang, Y., & Ren, J. (2021). Surface plasmon resonance study of the interaction between extracellular vesicles and cancer cells. *J. of Colloid and Interface Science*, **582**, 1247-1254. https://doi.org/10.1016/j.jcis.2020.09.125

Citation: Naim MR, Hossain M, Islam M, and Mitra S. (2023). Development of graphene with tungsten disulfide composite layer based SPR biosensor for biomedical application. *Aust. J. Eng. Innov. Technol.*, **5**(3), 119-129. https://doi.org/10.34104/ajeit.023.01190129